The influence of the geometric shape of the symmetrical twisted turbulator on the performance of parabolic solar collector having hybrid nanofluid: Numerical approach using two-phase model

Khalid H. Almitani [a], Ali Alzaed [b], Ahmad Alahmadi [c], Mohsen Sharifpur [d,e,*], Modaser Momin [d]

[a] Mechanical Engineering Department, Faculty of Engineering, King Abdulaziz University, Jeddah, Saudi Arabia
[b] Architectural Engineering Department, Faculty of Engineering, Taif University, Taif, Saudi Arabia
[c] Department of Electrical Engineering, College of Engineering, Taif University, Taif 21944, Saudi Arabia
[d] Department of Mechanical and Aeronautical Engineering, University of Pretoria, Pretoria, South Africa
[e] Department of Medical Research, China Medical University Hospital, China Medical University, Taichung 404, Taiwan

A R T I C L E I N F O

Keywords:
Twisted turbulators
Parabolic solar collector
Hybrid nanofluid
Exergy
Energy efficiency
Two-phase flow

A B S T R A C T

In this investigation, the influence of twisted turbulator and water-based MWCNT-MgO hybrid nanofluid on thermal–hydraulic performance (PEC), energy efficiency (η_n), and exergy efficiency (η_{ex}) of parabolic solar collectors (PSCs) was numerically investigated using the finite volume process. The two-phase nanofluid flows at the Reynolds number (Re) ranging of 10,000–25,000, the RNG k-ε turbulence model is used to model the turbulent flow regime. The nanofluid is modeled by a two-phase mixed model. In addition, the SIMPLEC algorithm was used for simulation. The study is performed for nanoparticles concentrations (φ) of 1% to 3% and pitch ratios (PR) of 0.25, 0.5, 0.75, and 1. Re and φ of MWCNT and MgO nanoparticles were detected to augments (Nu_{av}). It is detected that the values of PEC are more than 1 for all cases. Therefore, it can be concluded that using a twisted turbulator and an enhancement of its PR intensifies PEC. In addition, the results demonstrate that η_n is enhanced and η_{ex} is reduced with the PR of the solar collector having twisted. For case of φ = 3%, as Re increased from 10,000 to 25,000, $\eta_n$andη_{ex} are enhanced by 45.98% and 31.67% for PR = 1 and 0.25, respectively.

Introduction

An improvement of heat transfer rate (HTR) and efficiency in physical phenomena is of great importance today [1–3]. The main purpose in this field is to use techniques to enlarge efficiency [4–6], improve the HTR [7–10], enhance the efficiency of thermal equipment [11–14], and reduce the size of thermos-fluid devices [15–19]. Using various optimization methodology [20–22], artificial network [23], exergy analysis [24,25] as well as entropy generation [26–29] can be proceed to a better heat transfer. Another technique is the nanoparticles incorporation into fluid to vary the thermophysical properties such as thermal conductivity and viscosity [30–33] to enhance effectiveness [34–36].

Ghasemi and Ranjbar [37] numerically estimated the influence of porous rings on the PEC of a linear parabolic solar collector for Re of 7000 to 21000. They modeled turbulent flow by engaging the k-ε turbulent model. Their consequences have shown that porous rings advance the PEC of the linear PSC and enhance the Δp. Also, the maximum HTR was 49.51% at Re = 21000.

Goldanlou et al. [38] analytically modeled the impact of hybrid nanofluid on PEC of a PSC. They used the standard k-ε turbulence model. The authors showed that hybrid nanofluids' use causes a significant augmentation trendy on the PEC of the PSC compared to the base fluid. Also, Nu_{ave} enhances with φ and Re.

Nazir et al. [39] engaged water/alumina nanofluid in a PSC and measured the η_{ex} and η_n . They reported that the maximum enhancement in η_{ex} of the PSC is 23.11%.

Manjunath et al. [40] numerically, with the finite volume technique with the standard k-ε turbulence model, considered the influence of spherical generators on the heat transfer and fluid flow field on a solar heater. They showed that spherical vortex generators and enhancement in their height lead to an increase in the Nu_{ave}.

Sharafeldin and Grof [41] studied the influence of nanofluid having GeO_2 nanoparticle water-based fluid on the thermal performance of the solar collector experimentally and numerically. They experimentally fabricated water/GeO2 nanofluid using a two-step method. The

* Corresponding author at: Department of Mechanical and Aeronautical Engineering, University of Pretoria, Pretoria 0002, South Africa.
E-mail address: mohsen.sharifpur@up.ac.za (M. Sharifpur).

Nomenclature

Symbols	
c_P	Specific heat, (J/kgK)
D_h	Hydraulic diameter, (m)
D	Diameter of nanoparticles (nm)
F	Friction factor
k	Thermal conductivity, (W/mK)
Pr	Prandtl number
P	Pressure, (Pa)
T	Temperature (K)
U	Velocity *(m/s)*
Greek Symbols	
μ	Dynamic viscosity (mPa.s)
ρ	Density (m^3/kg)
φ	volume fraction (%)
Subscriptions	
bf	Base fluid
np	Nanoparticle
nf	Nanofluid
Abbreviations	
PEC	thermal–hydraulic performance
η_n	energy efficiency
η_{ex}	exergy efficiency
PTSC	Parabolic Trough Solar Collector
PR	pitch ratios
Re	Reynolds number

numerical part of their study was done using the computational fluid dynamics (CFD) method. They reported that the replacement of water/GeO_2 nanofluid in a solar collector improves its thermal performance. In addition, its thermal performance enhances with the φ of GeO_2 nanoparticles.

Kiliç et al. [42] considered the influence of AL_2O_3/water nanofluid inside a flat plate solar collector experimentally. They dispersed titanium oxide nanoparticles in water using a two-step technique. According to their experimental results, an increment in the φ of titanium oxide nanoparticles and Re improving the heat transfer of the flat panel solar collector.

Chamoli et al. [43] measured the effect of vortex generators in solar heaters numerically using CFD. The consequences indicated that the use of vortex generators and enhancement of the angle between them is directly related to the thermal performance of the solar heater. Also, the higher heat transfer enhancement in solar heater was 41.70%.

Rostami et al. [44] analytically considered the influence of the presence of an elliptical duct on the η_{ex} of a solar collector engaged with nanofluid having carbon nanotube water-base fluid using ANSYS FLUENT software, and finite volume process with k-ω turbulence model. The findings demonstrated that the use of an elliptical duct has a significant effect on the augmentation of the thermal performance of the solar collector. Besides, nanofluid is a more desirable base fluid in terms of thermal performance.

Milani Shirvan et al. [45] engaged finite volume technique to investigate the effect of single-phase and double-phase AL_2O_3/water nanofluid in a dual-pipe heat exchanger. They used a mixed model for modeling of two-phase nanofluid. Based on the results obtained from their study, the two-phase modeling of nanofluids leads to other appropriate predictions than the single-phase. Also, they revealed that Nu_{ave} was improved with Re and φ.

Ma et al. [46] studied the influence of two cold and hot heat sources in the space between two pipes. They revealed that two heat sources disrupt the shape of streamlines, leading to the generation of mixing and vortex formation, thus, an enhancement in the thermal performance.

Dezfulizadeh et al. [47] measured the influence of a novel turbulator and a magnetic field on the η_{ex} of a dual-pipe heat exchanger by engaging the finite volume technique and the standard k-ε turbulent model. According to the results, the use of the novel turbulators in a dual-pipe heat exchanger significantly enhances the η_{ex} compared to the heat exchanger without turbulators. Besides, the use of a magnetic field increased heat transfer.

Sheikholeslami et al. [48] numerically measured the influence of a twisted tape on the η_{ex} of double-phase nanofluid in a linear PSC. They used the Eulerian-Eulerian model to model two-phase nanofluids. According to the results, the η_{ex} depends on the PR of the twisted tape. Also, the maximum value of η_{ex} was 17.34%.

Using FLUENT software to analyze the fluid flow and finite volume method, Bellos et al. [49] observed the influence of helical turbulators on the PEC of copper oxide/water nanofluid in the PSC. It was established that helical turbulators leads to better heat performance than the PSC without turbulators. Furthermore, the higher heat performance of 56.78% was observed for a PSC.

Babaei Mahani et al. [50] examined the impact on a solar collector having twisted turbulators on the thermal transfer and fluid flow region of based-water MWCNT-AL_2O_3 hybrid nanofluid through a PSC using the finite volume method and FLUENT software. Their consequences showed that the simultaneous use of twisted turbulators and hybrid nanofluids significantly enhance Nu_{ave}. In addition, Nu_{ave} was enhanced with the curvature, φ, and Re.

According to previous studies, it can be concluded that the turbulator with the design of this study has not been used in PSCs. The application of this new geometry to a turbulator combined with a polymer hybrid nanofluid is also one of the innovations of this research. Also, the study of energy efficiency and exergy along with the coefficient of thermal–hydraulic performance at the same time has been studied in few studies. In the context of this literature review, the PEC, η_{ex} and η_n Two-phase MWCNT-MgO/water hybrid nanofluid flow in a solar collector equipped with twisted turbulators has not been studied. Therefore, the PEC of based- water MWCNT-MgO hybrid nanofluid with φ = 1 to 3%, Re = 10,000 to 25000, and PR = 0.25, 0.5, 0.75, and 1 is evaluated for turbulence flow regime.

Geometry of the model and equations

The geometry of the PSC with twisted turbulators is presented in Fig. 1. The tube length and the turbulator span are 800 mm and 300 mm, respectively. Moreover, the space between the twisted turbulator located in the middle of the absorber tube and the outlet and inlet is 250 mm. The surface-to-surface model is used for modeling the radiation. Also, to solve the turbulent flow, the RNG k-ε turbulent model and the SIMPLEC algorithm are used, respectively. A schematic of the twisted turbulator with dissimilar values of PR is shown in Fig. 2.

The characteristics of the PSC with twisted turbulators presented in Table 1.

The hybrid nanofluid of MWCNT-MgO/water was engaged as the working fluid. The thermophysical properties of MWCNT and MgO nanoparticles and the base fluid (water) are obtainable in Table 2.

The two-phase mixed method was engaged to simulate the based water MWCNT-MgO hybrid nanofluid flow within the solar collector. Also, the governing equations of the three-dimensional problem are [52–56]:

Continuity Eq:

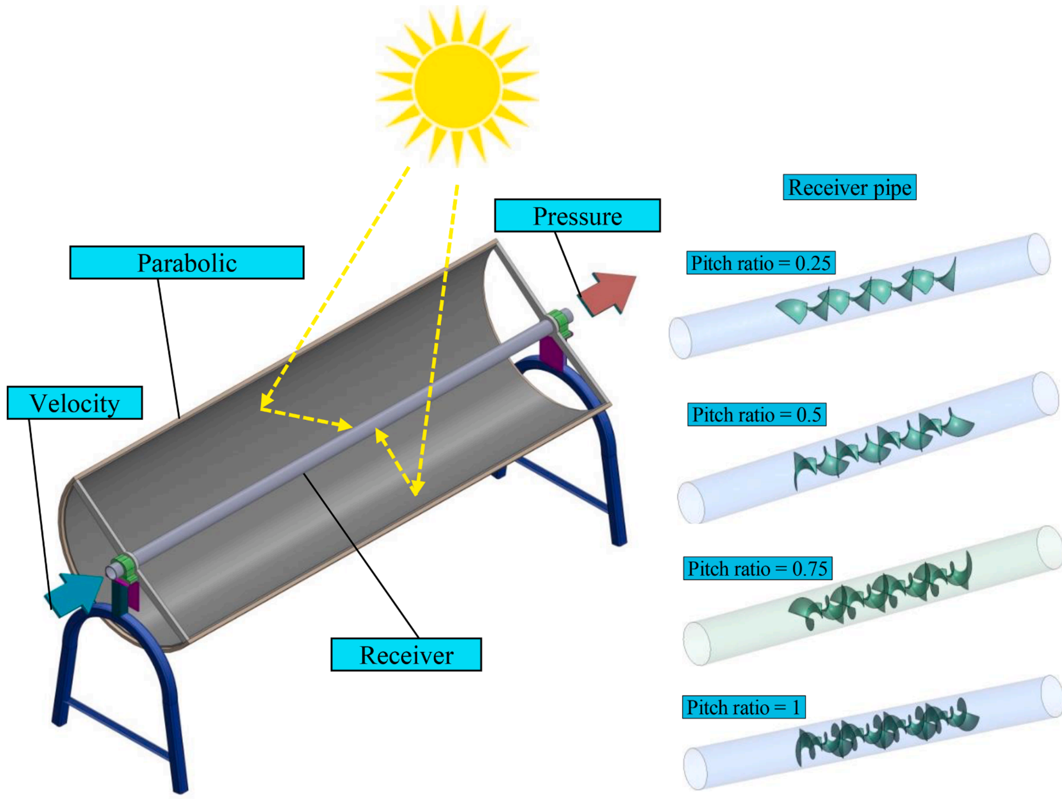

Fig. 1. Schematic of the geometry of a part of the solar collector with a twisted turbulator.

$$\frac{1}{r}\frac{\partial}{\partial\theta}(\rho u)+\frac{1}{r}\frac{\partial}{\partial r}(\rho r v)+\frac{\partial}{\partial\theta}(\rho w)=0 \tag{1}$$

Momentum Eq:

$$\frac{1}{r}\frac{\partial}{\partial\theta}(\rho uu)+\frac{1}{r}\frac{\partial}{\partial r}(\rho r vu)+\frac{\partial}{\partial z}(\rho wu)+\frac{1}{r}(\rho uv)=-\frac{1}{r}\frac{\partial P}{\partial\theta}+\frac{1}{r^2}\frac{\partial}{\partial\theta}\left(\mu\frac{\partial u}{\partial\theta}\right)+\frac{\partial}{\partial r}\left(\mu\frac{1}{r}\frac{\partial}{\partial r}(ru)\right)+2\mu\frac{1}{r^2}\frac{\partial v}{\partial\theta}+\rho g\beta(T_w-T)\sin\theta \tag{2}$$

$$\frac{1}{r}\frac{\partial}{\partial\theta}(\rho uv)+\frac{1}{r}\frac{\partial}{\partial r}(\rho r vv)+\frac{\partial}{\partial z}(\rho wv)-\frac{1}{r}(\rho u^2)=-\frac{1}{r}\frac{\partial P}{\partial\theta}+\frac{1}{r^2}\frac{\partial}{\partial\theta}\left(\mu\frac{\partial v}{\partial\theta}\right)+\frac{\partial}{\partial r}\left(\mu\frac{1}{r}\frac{\partial}{\partial r}(rv)\right)-2\mu\frac{1}{r^2}\frac{\partial u}{\partial\theta}-\rho g\beta(T_w-T)\cos\theta \tag{3}$$

$$\frac{1}{r}\frac{\partial}{\partial\theta}(\rho uw)+\frac{1}{r}\frac{\partial}{\partial r}(\rho r vw)+\frac{\partial}{\partial z}(\rho ww)=-\frac{\partial P}{\partial z}+\frac{1}{r^2}\frac{\partial}{\partial\theta}\left(\mu\frac{\partial w}{\partial\theta}\right)+\frac{1}{r}\frac{\partial}{\partial r}\left(r\mu\frac{\partial w}{\partial r}\right) \tag{4}$$

where r, θ, and z are the coordinates, u, v, and w are the velocity components.

Energy Eq:

$$\frac{1}{r}\frac{\partial}{\partial\theta}(\rho uT)+\frac{1}{r}\frac{\partial}{\partial r}(\rho r vT)+\frac{\partial}{\partial z}(\rho wT)=\frac{1}{r^2}\frac{\partial}{\partial\theta}\left(\frac{k}{c_p}\frac{\partial T}{\partial\theta}\right)+\frac{1}{r}\frac{\partial}{\partial r}\left(r\frac{k}{c_p}\frac{\partial T}{\partial r}\right) \tag{5}$$

$$\mathrm{Re}=\frac{\rho_f\bullet u_m\bullet D_i}{\mu_f} \tag{6}$$

The average Nusselt number is obtained from the following equation:

$$\mathrm{Nu}=\frac{h_f\bullet D_i}{k_f} \tag{7}$$

The Δp within the inlet to outlet of the test section is defined as:

$$\Delta P=P_{av,inlet}-P_{av,outlet} \tag{8}$$

Equation (9) is used to calculate the friction factor.

$$f=\frac{2}{\left(\frac{L}{D_i}\right)}\frac{\Delta P}{\rho_{nf}\bullet {u_m}^2} \tag{9}$$

Nanofluid properties including density, specific heat capacity, viscosity and thermal conductivity are obtained from Equations (10) to

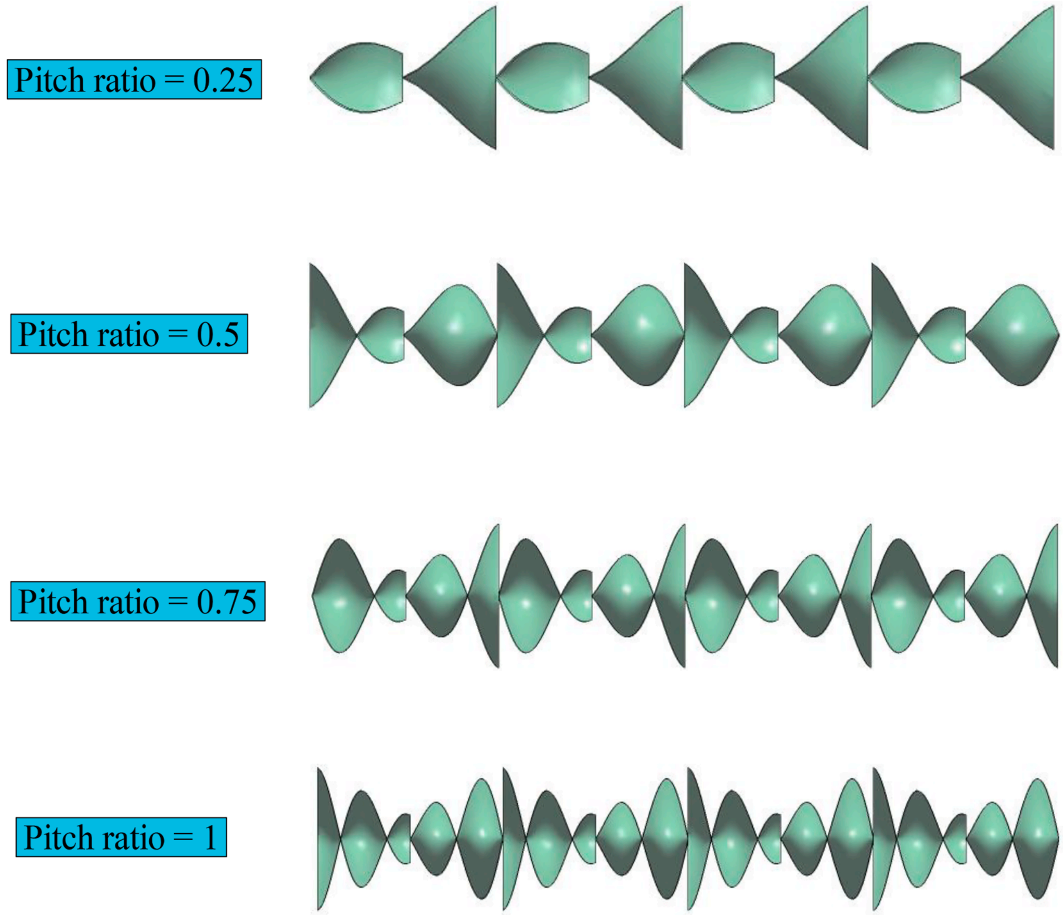

Fig. 2. Schematic of the twisted turbulator with different values of PR.

Table 1
Characteristics of the solar collector.

Value	Dimension
800 mm	L
50 mm	D
0.25, 0.5, 0.75, 1	PR

Table 2
Thermophysical properties of water, MgO and MWCNTs [50,51].

Property	MWCNT	MgO	Water
P (kg/m^3)	2100	3560	998.2
C_p (J/kgK	519	955	4182
k (W/mK	3000	45	0.6
μ (kg/ms)	–	–	0.001003

(13).

$$\rho_{nf} = \phi_{np1}\rho_{np1} + \phi_{np2}\rho_{np2} + \left(1 - \phi_{np1} - \phi_{np2}\right)\rho_{bf} \quad (10)$$

$$c_{p,nf} = \phi_{np1}c_{p,np} + \phi_{np2}c_{p,np2} + \left(1 - \phi_{np1} - \phi_{np2}\right)c_{p,bf} \quad (11)$$

$$\mu_{nf} = \frac{\mu_{bf}}{\left(1 - \phi_{np1} - \phi_{np2}\right)^{2.5}} \quad (12)$$

$$k_{nf} = k_f\left(\frac{(k_{np1} + k_{np2}) + 2k_f - 2\varphi_{np1}(k_f - k_{np1}) - 2\varphi_{np2}(k_f - k_{np2})}{(k_{np1} + k_{np2}) + 2k_f + \varphi_{np1}(k_f - k_{np1}) + \varphi_{np2}(k_f - k_{np2})}\right) \quad (13)$$

Energy and exergy efficiencies are obtained from Equations (14) and (15).

$$\eta_n = \frac{\frac{E_n}{I\bullet A} = p_{fo}\bullet Q_{in}\bullet \rho_{in}\bullet c_{p,in}\bullet\left(T_{fo,out} - T_{in}\right) + (1 - p_{fo})Q_{in}\bullet\rho_{in}\bullet c_{p,in}\bullet\left(T_{fi,out} - T_{in}\right)}{6\bullet 10^4\bullet I\bullet A} \quad (14)$$

$$\eta_{ex} = \frac{\dot{Q}_{HTF} - \dot{m}_{HTF}c_{p,HTF}\ln\left(\frac{T_\infty}{T_{i,HTF}}\right)}{-\dot{Q}_{HTF} - \dot{m}_{CF}c_{p,CF}\ln\left(\frac{T_{o,CF}}{T_{i,CF}}\right) + VI\eta_P} \quad (15)$$

While the mixture model has been used, it needs to indicate the equations that chose for property of the nanofluid.

Numerical modeling

In the current research, the finite volume technique and FLUENT software were employed to solve the governing equations. The geometry of the PSC was generated using SOLIDWORKS software. The grid of the geometry of a PSC was created by using ANSYS Mashing module. The three-dimensional solution and steady was optimized. The water/MWCNT-MgO hybrid nanofluid was simulated applying a two-phase mixed model. The flow is turbulent, and the RNG k-ε turbulence model was used to model the turbulent flow. Besides, to investigate the fluid flow behavior near a wall, the standard wall function is employed. The boundary condition at the inlet of the PSC is velocity inlet that leads to Re of 10,000 to 25,000. Also, φ = of 1 to 3% and PR = 0.25, 0.5, 0.75, and 1 are considered. The pressure outlet boundary condition is also used for the output of the PSC.

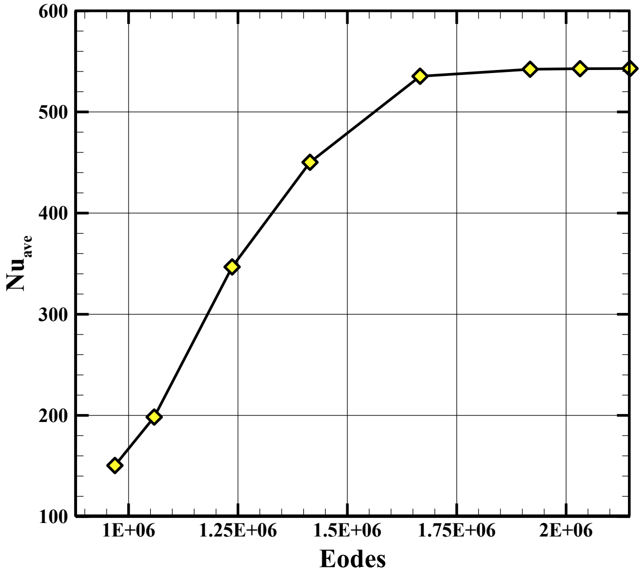

Fig. 3. Grid study results in terms of Nu_{ave} for MWCNT-MgO/water two-phase hybrid nanofluid within solar collector with twisted turbulator for Re = 25000, φ = 3%, and PR = 1.

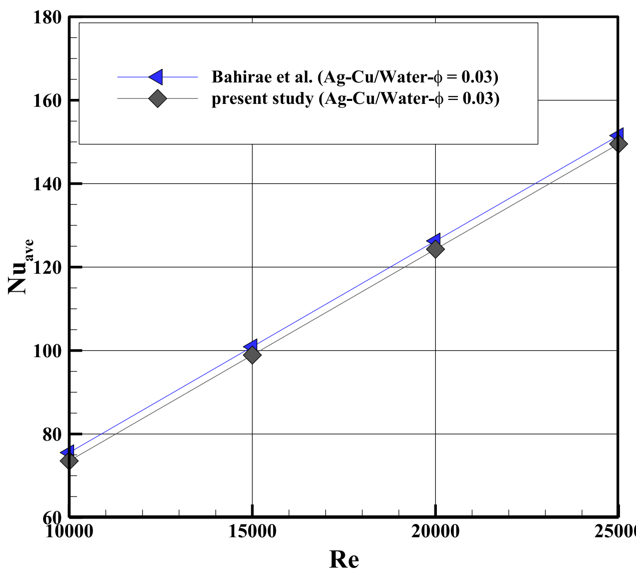

Fig. 4. Validation of the current numerical simulations with those of previous work.

Grid independence test

The grid study is performed to find a suitable grid for the present simulations. $Nu_{ave}$was calculated for MWCNT-MgO hybrid nanofluid flow within the solar collector with twisted turbulator for various grids (Fig. 3. According to the Figure, it can be concluded that the grid resolution of 2,031,769 is sufficient for the simulations because the further increase in the number of grid points does not change the value of Nu_{ave} significantly.

Validation

Validation of the current numerical results was approved using the model of Bahirai et al. [57] by calculating Nu_{ave} (Fig. 4. It can be noticed that the difference of 2.09% between the amounts of Nu_{ave} gained in the

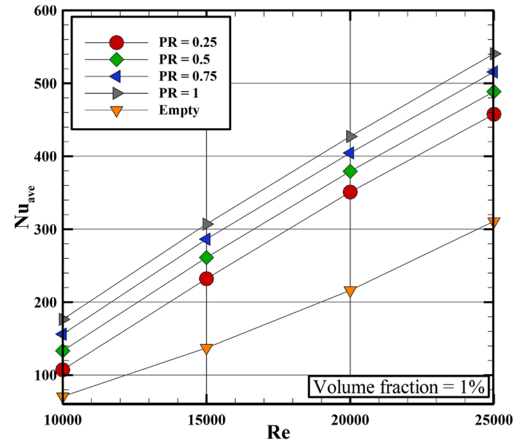

(a)

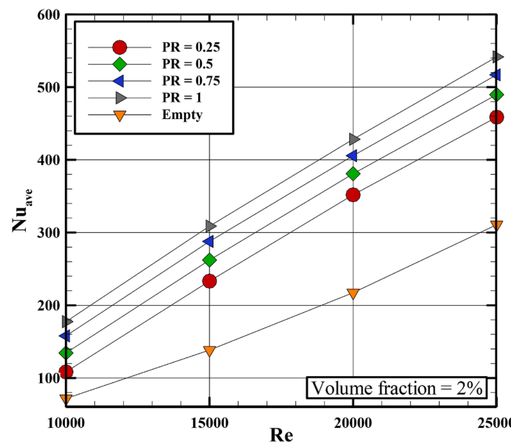

(b)

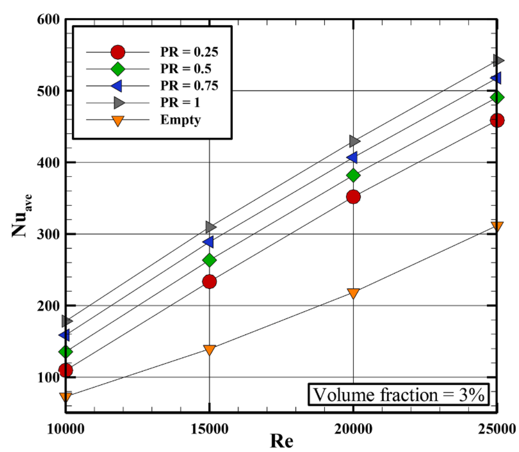

(c)

Fig. 5. Nu_{ave} in terms of Re of a PSC having a twisted turbulator with various values of PR and dissimilar nanoparticles concentrations.

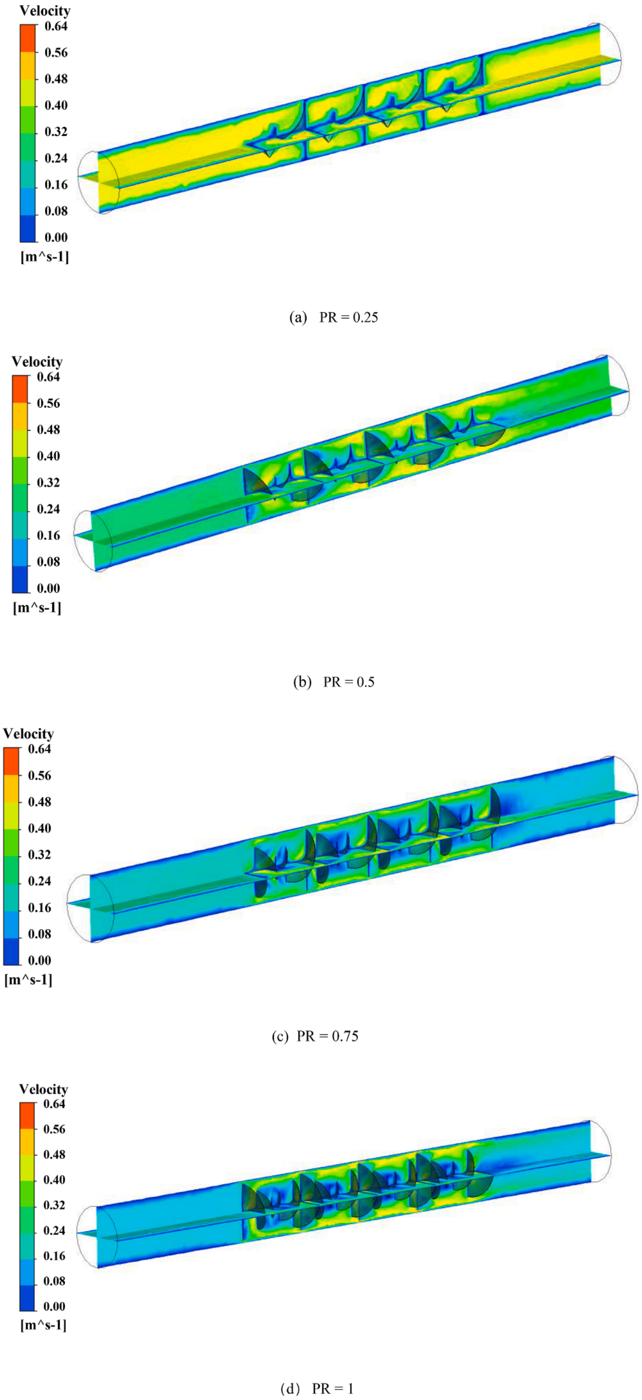

Fig. 6. Velocity contours for the two-phase MWCNT-MgO/water hybrid nanofluid flow with φ = 3% for Re = 25000.

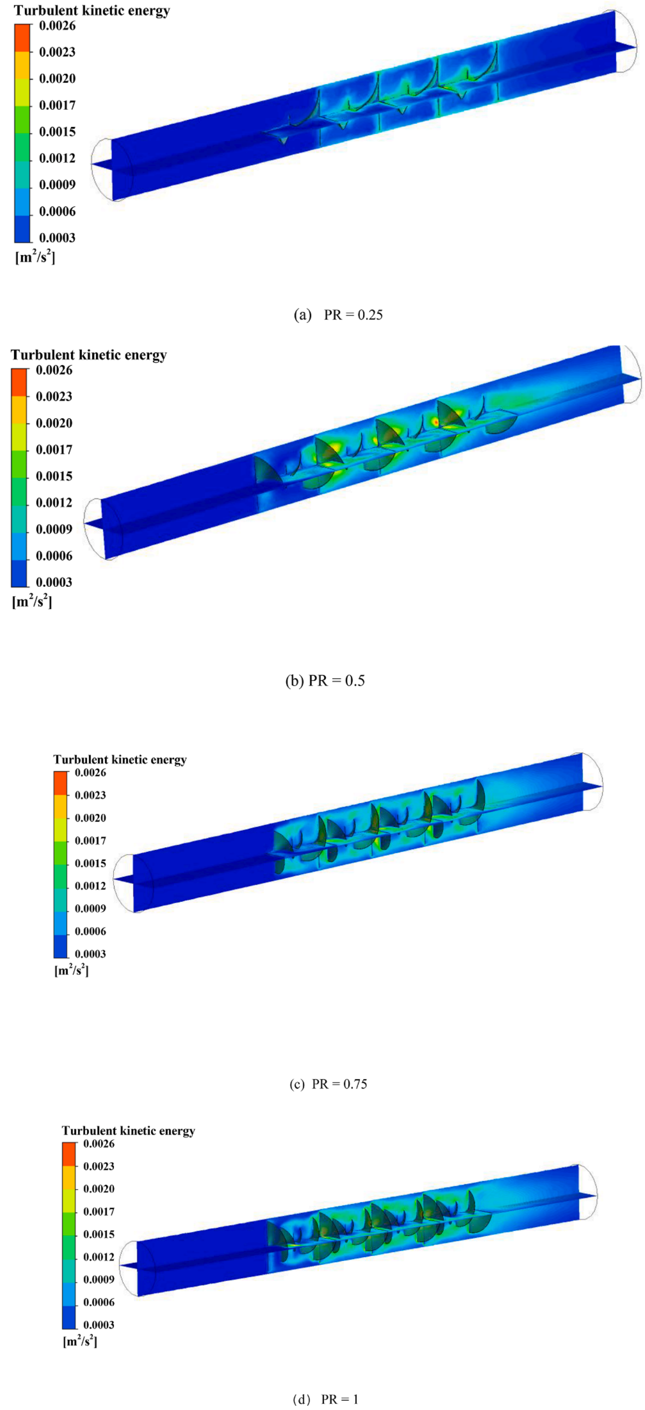

Fig. 7. Turbulent kinetic energy contours for two-phase MWCNT-MgO/water two-phase hybrid nanofluids with φ = 3% for Re = 25000.

current simulations and those of Bahirai et al. [57]. Hence, the accuracy of the modeling outcomes was confirmed.

Results and discussion

The present study results were presented for estimating the effect of turbulator and hybrid nanofluid on PEC, as well as η_n and η_{ex} of the PSC. The influence of different values of PR on Nu_{ave}, Δp, PEC, and η_n were examined. Moreover, the counters of velocity, turbulent kinetic energy, pressure, temperature, and streamlines inside the PSC with twisted turbulator are presented for PR = 0.25, 0.5, 0.75, and 1 when Re = 25000 and φ = 3%.

Influence of PR on Nu_{ave}

Fig. 5 demonstrates Nu_{ave} in terms of Re on a PSC having a twisted turbulator inside a PSC with different values of PR and different nanoparticles concentrations. As observed, an increment in the Re enhances the flow rate of the MWCNT-MgO/water hybrid nanofluid, causing the heat transfer coefficient to intensify and Nu_{ave} to enhance. As the Re rises, the HTR improves. Consequently, energy efficiency improves as heat exchange enhances. Also, an increase in the φ of MgO and MWCNT nanoparticles enhances the PEC of the PSC. At Re = 25,000, for cases of φ = 1%, 2% and 3%, the placement of twisted turbulators with PR = 1

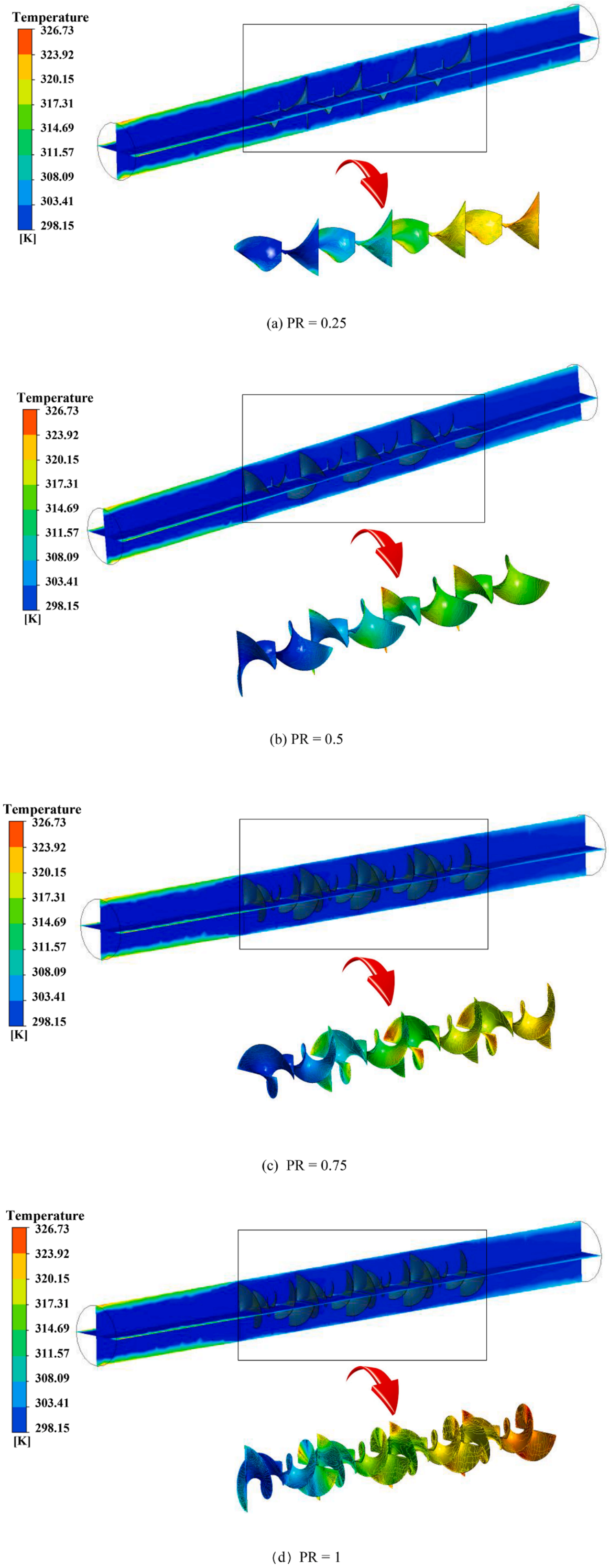

Fig. 8. Temperature contours for two-phase MWCNT-MgO/water two-phase hybrid nanofluids with φ = 3% for Re = 25000.

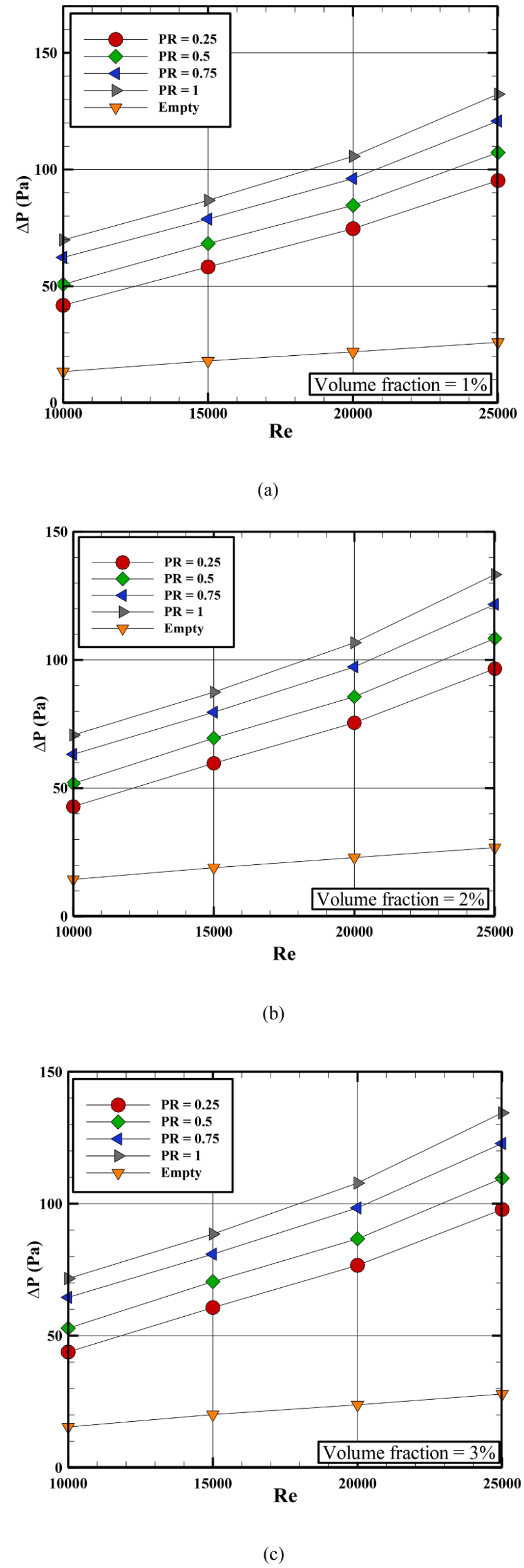

Fig. 9. Δp virsus Re in a PSC including a twisted turbulator with various values of PR and dissimilar nanoparticles concentrations.

respectively enhances Nu_{ave} by 68.11%, 69.70% and 71.25% compared to the PSC in the absence of turbulator.

Velocity contours for the two-phase MWCNT-MgO/water hybrid nanofluid flow with φ = 3% are shown in Fig. 6 for Re = 25000. As shown in the Figure, considering the no-slip boundary condition for the walls of the PSC, the velocity of the MWCNT-MgO/water two-phase hybrid nanofluid flow is zero near the wall. However, at the center of solar collector, the shape of the streamlines is disturbed due to the presence of a twisted turbulator, which causes the flow velocity in this area to be higher than near the wall.

The contours of turbulent kinetic energy are displayed in Fig. 7 (a, b, c, and d) for two-phase MWCNT-MgO/water two-phase hybrid nanofluids with φ = 3% for Re = 25000 and different PRs. Turbulent kinetic contours indicate areas where the intensity of turbulence is greater. With the help of turbulent kinetic contours, areas where there are more severe speed fluctuations can be well identified. As can be seen, turbulent kinetic energy is more significant in the areas between the surfaces of the twisted turbulator due to the creation of mixing and turbulence. Also, the intensity of turbulence enhances significantly with the PR.

Fig. 8 (a, b, c, and d) demonstrates the temperature contours for two-phase MWCNT-MgO/water two-phase hybrid nanofluids with φ = 3% for Re = 25000. As can be seen, the surface temperature of the turbulator is enhanced due to the collision of the nanofluid flow with the surface

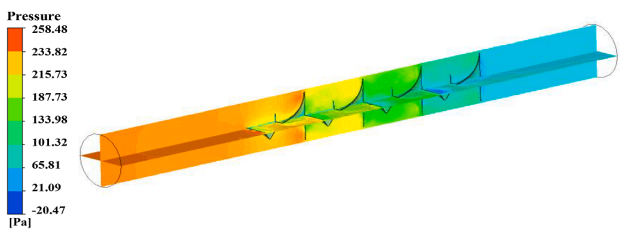

(a) PR = 0.5

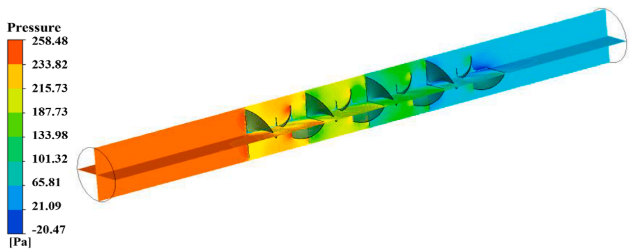

(b) PR = 0.5

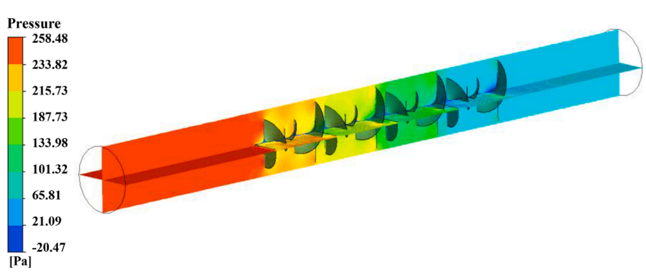

(c) PR = 0.75

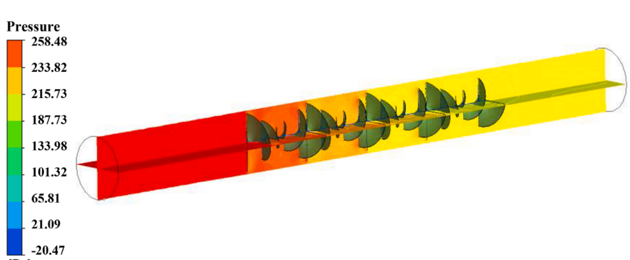

(d) PR = 1

Fig. 10. Pressure contours for two-phase MWCNT-MgO/water two-phase hybrid nanofluids with φ = 3% for Re = 25000.

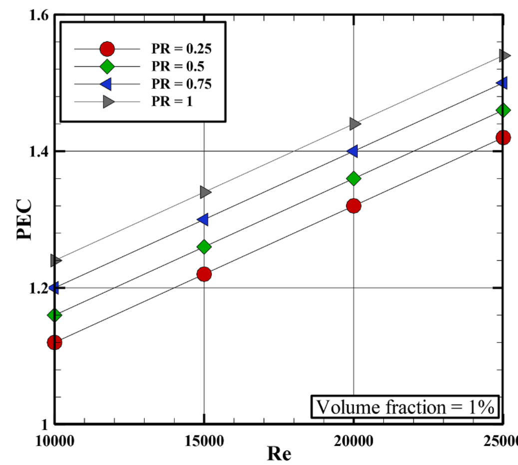

(a)

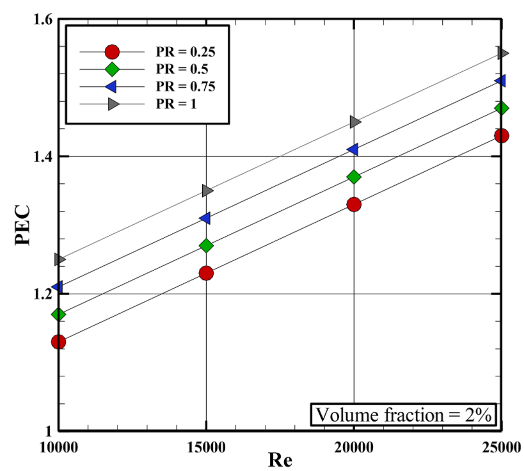

(b)

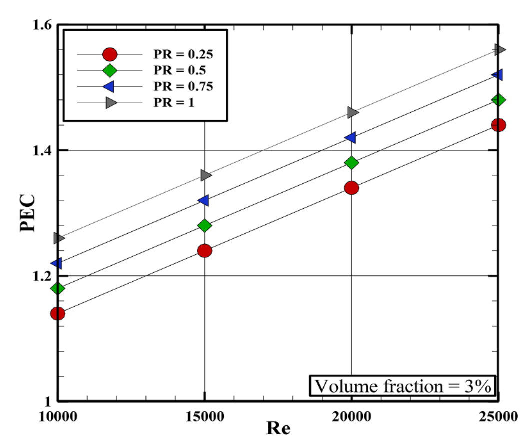

(c)

Fig. 11. PEC versus Re of the PSC equipped having a twisted turbulator at different values of PR for dissimilar nanoparticles concentrations.

and the effect of radiation.

Effect of PR on Δp

Fig. 9 shows Δp in subject of Re inside a PSC including a twisted turbulator at dissimilar values of PR and dissimilar nanoparticles concentrations. As can be seen, Δp is strongly influenced by Re, φ, and PR. As Re, φ, and PR enhance, the amount of Δp is intensified. At Re = 25,000 and φ = 1%, the twisted turbulator with PR = 1 augments the Δp by 385.19% in comparison of the PSC without turbulator. At Re = 25,000 and φ = 2%, the twisted turbulator with PR = 1 increases the Δp by 387.09% in comparison of the PSC without turbulator. At Re = 25,000 and φ = 3%, the twisted turbulator with PR = 1 enhances the Δp by 388.59% in comparison of the PSC without turbulator.

The contours of pressure are illustrated in Fig. 10 (a, b, c, and d) for two-phase MWCNT-MgO/water two-phase hybrid nanofluids with φ = 3% for Re = 25000. As can be seen, similar to the results reported by other researchers, the placement of the turbulator causes the streamlines to be dense, resulting in mixing and turbulence. Therefore, the Δp is very high at the moment of collision of two-phase MWCNT-MgO/water hybrid nanofluid with a twisted turbulator. However, the value of Δp is reduced along with the solar collector for all cases.

Effect of PR on PEC

The changes in PEC versus Re of the PSC containing a twisted turbulator with dissimilar values of PR for dissimilar nanoparticles concentrations are presented in Fig. 11. As can be seen, the amounts of the PEC coefficient are more than 1 for all cases. Therefore, it can be found that the presence of a twisted turbulator and an augmentation in PR improves the PEC.

The contours of streamline are given in Fig. 12 for MWCNT-MgO/water hybrid nanofluids with φ = 3% for Re = 25000. As observed, the concentration of the streamlines was enhanced with the PR.

Effect of PR on η_n

Fig. 13 (a, b, c, and d) reveals the amount of η_n versus Re of the PSC equipped having a twisted turbulator at different values of φ and PR = (0.25, 0.5, 0.75 and 1). As can be seen, the η_n is strongly influenced by Re, φ, and PR for all cases. At φ = 3%, by intensifying the Re from 10,000 to 25,000, value of η_n was enhanced by 42.11%, 43.87%, 45.16% and 45.98% for PR = 0.25, 0.5, 0.75 and 1, respectively.

Effect of PR on η_{ex}

The variation of η_{ex} in terms of Re is displayed in Fig. 14. The PSC containing a twisted turbulator at dissimilar amounts of φ and PR = (0.25, 0.5, 0.75 and 1). As can be seen from the results, η_{ex} is an ascensional function with Re and φ and a decreasing function with PR. As the PR ratio decreases, the exergy efficiency intensifies. One of the factors affecting the exergy efficiency is the HTR. As the PR ratio diminishes, the turbulence of the flow decreases as a result of the heat exchange between the nanofluid particles; therefore, the exergy efficiency decreases. Also, with growing volume fraction, the exergy efficiency augments. As mentioned above, one of the factors affecting the exergy efficiency is the HTR. As the volume fraction intensifies, the thermal conductivity of the nanofluid rises, resulting in improved heat exchange and augmented exergy efficiency.

In a PSC having a twisted turbulator, containing nanofluid at φ = 3%,

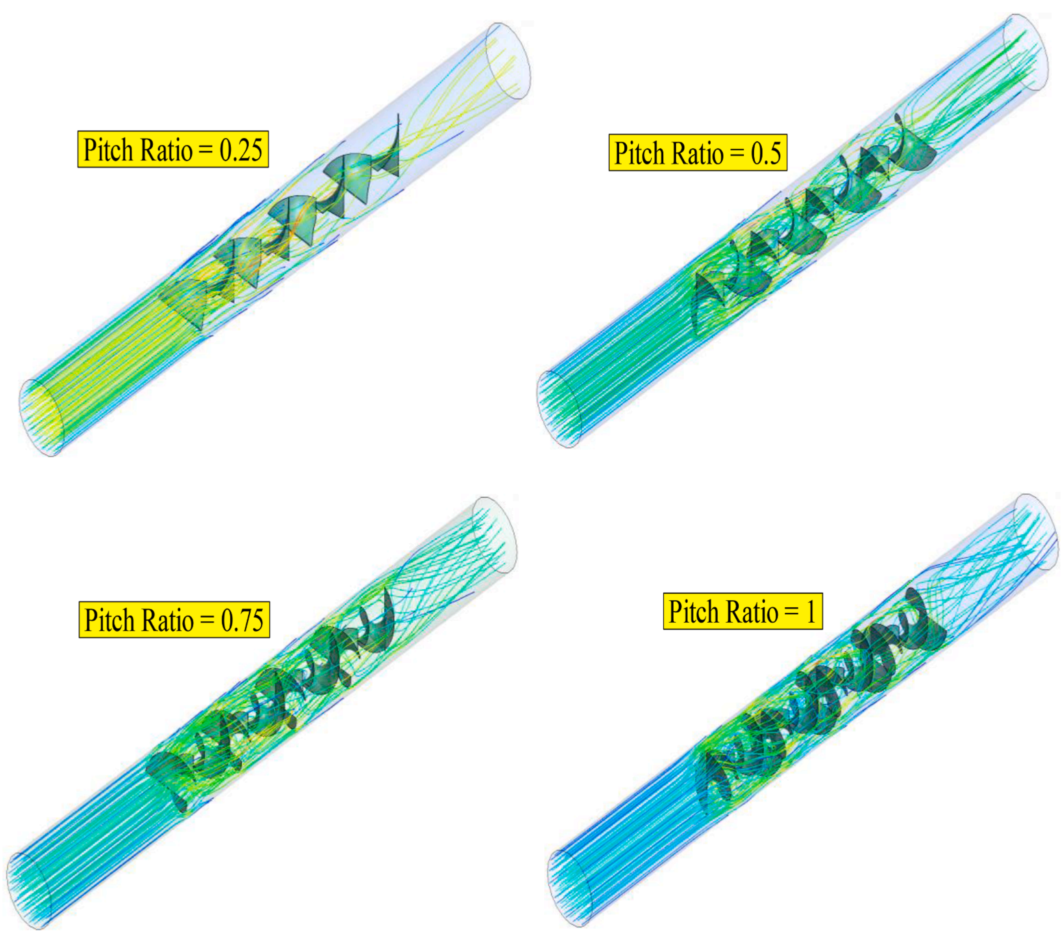

Fig. 12. The streamline contours MWCNT-MgO/water hybrid nanofluids at φ = 3% for Re = 25000.

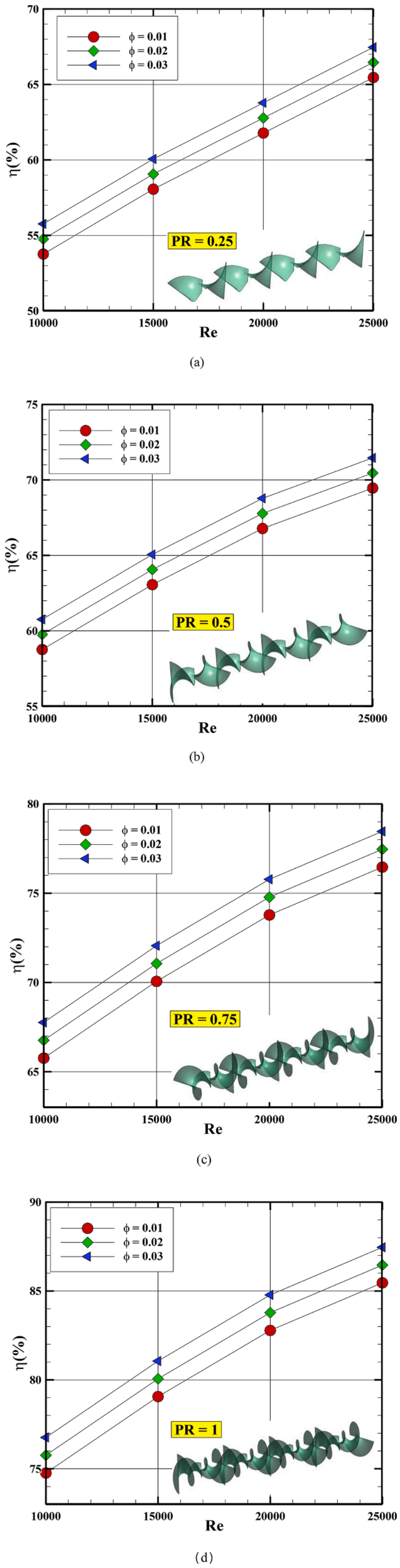

Fig. 13. The amount of η_n versus Re inside a PSC containing a twisted turbulator at dissimilar values of φ and PR.

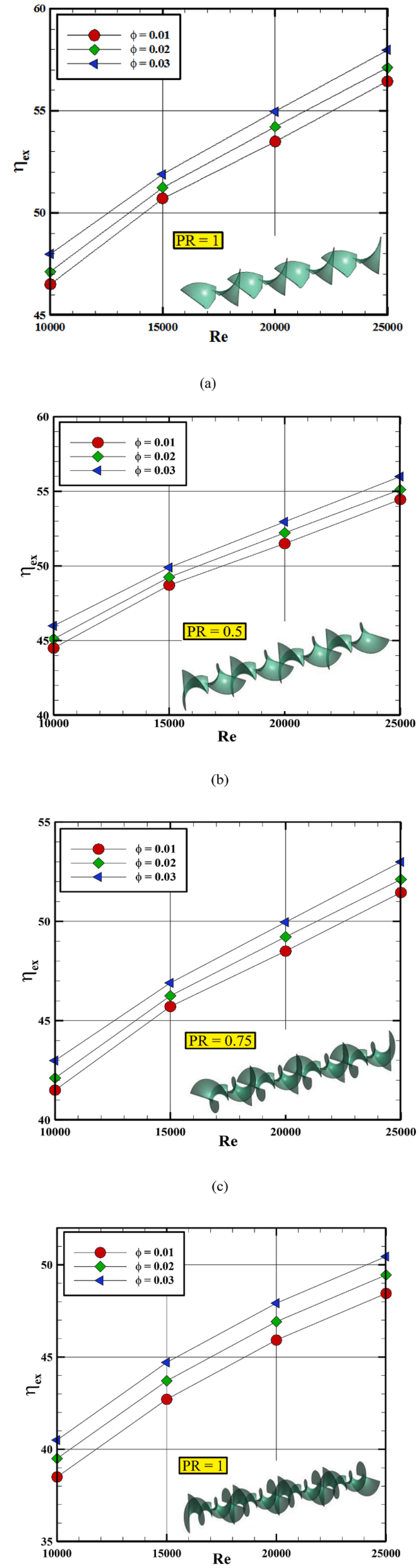

Fig. 14. The variation of η_{ex} in terms of Re of the PSC equipped having a twisted turbulator with dissimilar amounts of φ and PR.

by intensifying the Re from 10,000 to 25,000, value of η_{ex} was increased by 31.67%, 30.13%, 30.02% and 29.87% for PR = 0.25, 0.5, 0.75 and 1, respectively.

Conclusions

In the current research, the influence of twisted turbulator and two-phase MWCNT- MgO_2/water hybrid nanofluid on PEC, η_n, and η_{ex} of the PSC was evaluated numerically employing the finite volume method and

FLUENT software. Since 10,000 < Re < 25,000, the RNG k-ε turbulence model was used to model the turbulent flow. The nanofluid was modeled by using a two-phase mixed model. In addition, the SIMPLEC algorithm was employed to discretize the equations. The study was performed for φ = 1 to 3% and PR = 0.25, 0.5, 0.75, and 1 inside a PSC. According to the results:

- The Nuave enhances with Re and φ of MWCNT and MgO nanoparticles.
- The Δp in the PSC is enhanced with Re and φ of MWCNT and MgO nanoparticles.
- The Nuave and Δp intensify significantly with PR of the twisted turbulator.
- For the case of Re = 25,000 and φ = 3% and, the presence of twisted turbulators with PR = 1 augments Nuave and Δp by 71.25% and 388.59%, respectively, in comparison of the PSC without turbulator.
- The results revealed that the amounts of PEC are more than 1 for all cases. Therefore, it can be concluded that the presence of a twisted turbulator and increasing its PR intensify PEC.
- By increasing the PR of a twisted turbulator inside a PSC, η_n is enhanced and η_{ex} is reduced.
- For case of φ = 3%, as Re increased from 10,000 to 25,000, ηn and ηex are enhanced by 45.98% and 31.67% for PR = 1 and 0.25, respectively.

CRediT authorship contribution statement

Khalid H. Almitani: Conceptualization, Writing – original draft. **Ali Alzaed:** Validation, Software. **Ahmad Alahmadi:** Writing – review & editing. **Mohsen Sharifpur:** Conceptualization, Writing – review & editing. **Modaser Momin:** Writing – review & editing.

Declaration of Competing Interest

The authors declare that they have no known competing financial interests or personal relationships that could have appeared to influence the work reported in this paper.

Acknowledgment

Authors would like to thank Taif University, Researchers Support Project Number (TURSP-2020/240) Taif University, Taif, Saudi Arabia.

References

[1] Shahsavar Goldanlou A, Kalbasi R, Afrand M. Energy usage reduction in an air handling unit by incorporating two heat recovery units. J Building Eng 2020;32:101545.
[2] Afrand M, Farahat S, Nezhad AH, Sheikhzadeh GA, Sarhaddi F, Wongwises S. Multi-objective optimization of natural convection in a cylindrical annulus mold under magnetic field using particle swarm algorithm. Int Commun Heat Mass Transfer 2015;60:13–20.
[3] Alizadeh R, Karimi N, Mehdizadeh A, Nourbakhsh A. Analysis of transport from cylindrical surfaces subject to catalytic reactions and non-uniform impinging flows in porous media. J Therm Anal Calorim 2019;138:659–78.
[4] Afrand M, Farahat S, Nezhad AH, Sheikhzadeh GA, Sarhaddi F. Numerical simulation of electrically conducting fluid flow and free convective heat transfer in an annulus on applying a magnetic field. Heat Transfer Research 2014;45.
[5] Manirathnam AS, Dhanush Manikandan MK, Hari Prakash R, Kamesh Kumar B, Deepan Amarnath M. Experimental analysis on solar water heater integrated with Nano composite phase change material (SCi and CuO). Mater Today: Proc 2021;37:232–40.
[6] Rahmani E, Moradi T, Fattahi A, Delpisheh M, Karimi N, Ommi F, et al. Numerical simulation of a solar air heater equipped with wavy and raccoon-shaped fins: The effect of fins' height. Sustainable Energy Technol Assess 2021;45:101227.
[7] Kaushal R, Kumar R. Heat Transfer Enhancement Using Augmented Tubes for Desalination Using Fuzzy-TOPSIS Approach. Renewable Energy Res Appl 2020;1:19–26.
[8] Alizadeh R, Karimi N, Nourbakhsh A. Effects of radiation and magnetic field on mixed convection stagnation-point flow over a cylinder in a porous medium under local thermal non-equilibrium. J Therm Anal Calorim 2020;140:1371–91.
[9] Habib R, Karimi N, Yadollahi B, Doranehgard MH, Li LK. A pore-scale assessment of the dynamic response of forced convection in porous media to inlet flow modulations. Int J Heat Mass Transf 2020;153:119657.
[10] Saeed A, Karimi N, Paul MC. Analysis of the unsteady thermal response of a Li-ion battery pack to dynamic loads. Energy 2021;231:120947.
[11] Yari M, Kalbasi R, Talebizadehsardari P. Energetic-exergetic analysis of an air handling unit to reduce energy consumption by a novel creative idea. Int J Numer Meth Heat Fluid Flow 2019;29:3959–75.
[12] Akhtari MR, Shayegh I, Karimi N. Techno-economic assessment and optimization of a hybrid renewable earth-air heat exchanger coupled with electric boiler, hydrogen, wind and PV configurations. Renewable Energy 2020;148:839–51.
[13] Habib R, Yadollahi B, Karimi N, Doranegard MH. On the unsteady forced convection in porous media subject to inlet flow disturbances-A pore-scale analysis. Int Commun Heat Mass Transfer 2020;116:104639.
[14] Zhang X, Tang Y, Zhang F, Lee CS. A novel aluminum–graphite dual-ion battery. Adv Energy Mater 2016;6:1502588.
[15] Mortazavi SM, Garoosi S. Role of Energy Supply and demand Fluctuations in Macroeconomic Development of Iran. Renewable Energy Res Appl 2020;1:85–92.
[16] Ghazvini M, Pourkiaei S, Pourfayaz F. Thermo-Economic Assessment and Optimization of Actual Heat Engine Performance by Implemention of NSGA II. Renewable Energy Res Appl 2020;1:235–45.
[17] Salimpour MR, Kalbasi R, Lorenzini G. Constructal multi-scale structure of PCM-based heat sinks. Continuum Mech Thermodyn 2017;29:477–91.
[18] Hunt G, Karimi N, Mehdizadeh A. Intensification of ultra-lean catalytic combustion of methane in microreactors by boundary layer interruptions–A computational study. Chem Eng Sci 2021;242:116730.
[19] Ariyo DO, Bello-Ochende T. Critical heat fluxes for subcooled flow boiling in optimised microchannels. Int J Hydromechatronics 2020;3:140–54.
[20] Cai T, Zhao D, Karimi N. Optimizing thermal performance and exergy efficiency in hydrogen-fueled meso-combustors by applying a bluff-body. J Cleaner Prod 2021;311:127573.
[21] Kandilli C, Mertoglu B. Optimisation design and operation parameters of a photovoltaic thermal system integrated with natural zeolite. Int J Hydromechatronics 2020;3:128–39.
[22] Li X, Gui D, Zhao Z, Li X, Wu X, Hua Y, et al. Operation optimization of electrical-heating integrated energy system based on concentrating solar power plant hybridized with combined heat and power plant. J Cleaner Prod 2021;289:125712.
[23] J. Mohebbi Najm Abad, R. Alizadeh, A. Fattahi, M. H. Doranehgard, E. Alhajri, and N. Karimi, "Analysis of transport processes in a reacting flow of hybrid nanofluid around a bluff-body embedded in porous media using artificial neural network and particle swarm optimization," *Journal of Molecular Liquids,* vol. 313, p. 113492, 2020/09/01/ 2020.
[24] Liu W, Kalbasi R, Afrand M. Solutions for enhancement of energy and exergy efficiencies in air handling units. J Cleaner Prod 2020;257:120565.
[25] Wang L, Izaharuddin AN, Karimi N, Paul MC. A numerical investigation of CO2 gasification of biomass particles- analysis of energy, exergy and entropy generation. Energy 2021;228:120615.
[26] Gomari SR, Alizadeh R, Alizadeh A, Karimi N. Generation of entropy during forced convection of heat in nanofluid stagnation-point flows over a cylinder embedded in porous media. Numerical Heat Transfer, Part A: Applications 2019;75:647–73.
[27] Guthrie DGP, Torabi M, Karimi N. Energetic and entropic analyses of double-diffusive, forced convection heat and mass transfer in microreactors assisted with nanofluid. J Therm Anal Calorim 2019;137:637–58.
[28] Christodoulou L, Karimi N, Cammarano A, Paul M, Navarro-Martinez S. State prediction of an entropy wave advecting through a turbulent channel flow. J Fluid Mech 2019;882:A8.
[29] Govone L, Torabi M, Hunt G, Karimi N. Non-equilibrium thermodynamic analysis of double diffusive, nanofluid forced convection in catalytic microreactors with radiation effects. Entropy 2017;19:690.
[30] Nwosu PN, Meyer J, Sharifpur M. Nanofluid Viscosity: A simple model selection algorithm and parametric evaluation. Comput Fluids 2014;101:241–9.
[31] Ranjbarzadeh R, Akhgar A, Musivand S, Afrand M. Effects of graphene oxide-silicon oxide hybrid nanomaterials on rheological behavior of water at various time durations and temperatures: Synthesis, preparation and stability. Powder Technol 2018;335:375–87.
[32] Hemmat Esfe M, Abbasian Arani AA, Esfandeh S, Afrand M. Proposing new hybrid nano-engine oil for lubrication of internal combustion engines: Preventing cold start engine damages and saving energy. Energy 2019;170:228–38.
[33] Ghasemi A, Hassani M, Goodarzi M, Afrand M, Manafi S. Appraising influence of COOH-MWCNTs on thermal conductivity of antifreeze using curve fitting and neural network. Physica A 2019;514:36–45.
[34] Li Z, Sarafraz M, Mazinani A, Hayat T, Alsulami H, Goodarzi M. Pool boiling heat transfer to CuO-H2O nanofluid on finned surfaces. Int J Heat Mass Transf 2020;156:119780.
[35] Bahiraei M, Jamshidmofid M, Goodarzi M. Efficacy of a hybrid nanofluid in a new microchannel heat sink equipped with both secondary channels and ribs. J Mol Liq 2019;273:88–98.
[36] Tee KF. The influence of water on frequency response of concrete plates armed by nanoparticles utilising analytical approach. Int J Hydromechatronics 2020;3:51–68.
[37] Ghasemi SE, Ranjbar AA. Numerical thermal study on effect of porous rings on performance of solar parabolic trough collector. Appl Therm Eng 2017;118:807–16.
[38] Goldanlou AS, Sepehrirad M, Dezfulizadeh A, Golzar A, Badri M, Rostami S. Effects of using ferromagnetic hybrid nanofluid in an evacuated sweep-shape solar receiver. J Therm Anal Calorim 2021;143:1623–36.

[39] Nazir MS, Ghasemi A, Dezfulizadeh A, Abdalla AN. Numerical simulation of the performance of a novel parabolic solar receiver filled with nanofluid. J Therm Anal Calorim 2021;144:2653–64.
[40] Manjunath M, Karanth KV, Sharma NY. Numerical analysis of the influence of spherical turbulence generators on heat transfer enhancement of flat plate solar air heater. Energy 2017;121:616–30.
[41] Sharafeldin M, Grof G. Evacuated tube solar collector performance using CeO2/water nanofluid. J Cleaner Prod 2018;185:347–56.
[42] Kiliç F, Menlik T, Sözen A. Effect of titanium dioxide/water nanofluid use on thermal performance of the flat plate solar collector. Sol Energy 2018;164:101–8.
[43] Chamoli S, Lu R, Xu D, Yu P. Thermal performance improvement of a solar air heater fitted with winglet vortex generators. Sol Energy 2018;159:966–83.
[44] Rostami S, Sepehrirad M, Dezfulizadeh A, Hussein AK, Shahsavar Goldanlou A, Shadloo MS. Exergy optimization of a solar collector in flat plate shape equipped with elliptical pipes filled with turbulent nanofluid flow: A study for thermal management. Water 2020;12:2294.
[45] Shirvan KM, Mamourian M, Mirzakhanlari S, Ellahi R. Numerical investigation of heat exchanger effectiveness in a double pipe heat exchanger filled with nanofluid: a sensitivity analysis by response surface methodology. Powder Technol 2017;313:99–111.
[46] Ma Y, Jamiatia M, Aghaei A, Sepehrirad M, Dezfulizadeh A, Afrand M. Effect of differentially heated tubes on natural convection heat transfer in a space between two adiabatic horizontal concentric cylinders using nano-fluid. Int J Mech Sci 2019;163:105148.
[47] Dezfulizadeh A, Aghaei A, Joshaghani AH, Najafizadeh MM. Exergy efficiency of a novel heat exchanger under MHD effects filled with water-based Cu–SiO 2-MWCNT ternary hybrid nanofluid based on empirical data. J Therm Anal Calorim 2021:1–24.
[48] Sheikholeslami M, Jafaryar M, Abohamzeh E, Shafee A, Babazadeh H. Energy and entropy evaluation and two-phase simulation of nanoparticles within a solar unit with impose of new turbulator. Sustainable Energy Technol Assess 2020;39:100727.
[49] Bellos E, Tzivanidis C, Tsimpoukis D. Enhancing the performance of parabolic trough collectors using nanofluids and turbulators. Renew Sustain Energy Rev 2018;91:358–75.
[50] Mahani RB, Hussein AK, Talebizadehsardari P. Thermal–hydraulic performance of hybrid nano-additives containing multiwall carbon nanotube-Al2O3 inside a parabolic through solar collector with turbulators. Math Methods Appl Sci 2020.
[51] Davarnejad R, Jamshidzadeh M. CFD modeling of heat transfer performance of MgO-water nanofluid under turbulent flow. Eng Sci Technol, Int J 2015;18:536–42.
[52] Sadripour S, Chamkha AJ. The effect of nanoparticle morphology on heat transfer and entropy generation of supported nanofluids in a heat sink solar collector. Thermal Sci Eng Progress 2019;9:266–80.
[53] Ansys I. ANSYS CFX Release. "Ansys CFX-Solver Theory Guide. 2009,";11.
[54] Behzadmehr A, Saffar-Avval M, Galanis N. Prediction of turbulent forced convection of a nanofluid in a tube with uniform heat flux using a two phase approach. Int J Heat Fluid Flow 2007;28:211–9.
[55] Hejazian M, Moraveji MK, Beheshti A. Comparative study of Euler and mixture models for turbulent flow of Al2O3 nanofluid inside a horizontal tube. Int Commun Heat Mass Transfer 2014;52:152–8.
[56] Göktepe S, Atalık K, Ertürk H. Comparison of single and two-phase models for nanofluid convection at the entrance of a uniformly heated tube. Int J Therm Sci 2014;80:83–92.
[57] Bahiraei M, Mazaheri N, Moayedi H. Employing V-shaped ribs and nanofluid as two passive methods to improve second law characteristics of flow within a square channel: A two-phase approach. Int J Heat Mass Transf 2020;151:119419.